JGR Planets

RESEARCH ARTICLE
10.1029/2020JE006423

Key Points::

- Varying geochemical parameters of iron redox state, pH, and ammonia concentration affect the outcome of an organic reaction network
- Organic pattern distributions produced abiotically in geological systems are not random and vary depending on the geochemical conditions
- Environmental conditions affect the relative amounts of organics formed in this mineral system, which has implications for biosignature detection and prebiotic chemistry

Supporting Information:

- Supporting Information S1
- Table S1

Correspondence to:

L. M. Barge,
laura.m.barge@jpl.nasa.gov

Citation:

Barge, L. M., Flores, E., VanderVelde, D. G., Weber, J. M., Baum, M. M., & Castonguay A. (2020). Effects of geochemical and environmental parameters on abiotic organic chemistry driven by iron hydroxide minerals. *Journal of Geophysical Research: Planets*, *125*, e2020JE006423. https://doi.org/10.1029/2020JE006423

Received 20 FEB 2020
Accepted 5 OCT 2020

Effects of Geochemical and Environmental Parameters on Abiotic Organic Chemistry Driven by Iron Hydroxide Minerals

L. M. Barge[1], E. Flores[1], D. G. VanderVelde[2], J. M. Weber[1], M. M. Baum[3], and A. Castonguay[3]

[1]NASA Jet Propulsion Laboratory, California Institute of Technology, Pasadena, CA, USA, [2]Department of Chemistry, California Institute of Technology, Pasadena, CA, USA, [3]Department of Chemistry, Oak Crest Institute of Science, Monrovia, CA, USA

Abstract Geological conditions play a significant role in prebiotic/abiotic organic chemistry, especially when reactive minerals are present. Previous studies of the prebiotic synthesis of amino acids and other products in mineral-containing systems have shown that a diverse array of compounds can be produced, depending on the experimental conditions. However, these previous experiments have not simulated the effects of varying geochemical conditions, in which factors such as pH, iron redox state, or chemical concentrations may vary over time and space in a natural environment. In geochemical systems that contain overlapping gradients, many permutations of individual conditions could exist and affect the outcome of an organic reaction network. We investigated reactions of pyruvate and glyoxylate, two compounds that are central to the emergence of metabolism, in simulated geological gradients of redox, pH, and ammonia concentration. Our results show that the positioning of pyruvate/glyoxylate reactions in this environmental parameter space determines the organic product distribution that results. Therefore, the distribution pattern of amino acids and alpha-hydroxy acids produced prebiotically in a system reflects the specific reaction conditions, and would be distinct at various locations in an environment depending on local geochemistry. This is significant for origin of life chemistry in which the composition and function of oligomers could be affected by the environmentally driven distribution of monomers available. Also, for astrobiology and planetary science where organic distribution patterns are sometimes considered as a possible biosignature, it is important to consider environmentally driven abiotic organic reactions that might produce similar effects.

Plain Language Summary To understand the potential for life elsewhere, it is important to try to find organic molecules on other planets, but also to understand the "pattern distributions" of organics–that is, the relative amounts of different organic molecules in a system. It is possible that organic distribution patterns could be a biosignature, but only if they can be deconvoluted from nonbiological organic chemistry. We conducted lab simulations of abiotic organic reactions (of important prebiotic molecules) in systems containing reactive iron minerals, similar to conditions that might exist in a variety of planetary environments as well as the early Earth when life emerged. We studied the distributions of products that are formed in this reaction as a function of conditions that would exist in geological environments, and found that different amounts of specific organic products were formed depending on the starting conditions. Our findings illustrate how, even in nonbiological systems, there is a lot of variety in the outcomes of organic chemical reactions and it is important to fully characterize abiotic systems to be able to identify systems that might contain life.

1. Introduction

Determining the role of geological environments in the synthesis of organic molecules is an important challenge for origin of life research as well as for understanding how to deconvolute abiotic signatures from biological signatures in planetary missions. For understanding how the emergence of metabolism could have occurred in a geological environment, much work focuses on studying reactions of organic molecules that are both important to modern biology and also are likely to have been present at life's origin. Pyruvate and glyoxylate are two carboxylic acid compounds that are of particular prebiotic interest: They are central to modern biochemistry, can be synthetized abiotically (Cody et al., 2000; Echkardt et al., 2019; Eggins et al.,

1988; Marín-Yaseli et al., 2016; Mohammed et al., 2017; Varma et al., 2018), and can lead into a variety of important reaction pathways for origin of life including reactions that resemble ancient proto-metabolic cycles (Muchowska et al., 2017, 2019). In previous studies, pyruvate and/or glyoxylate have been shown to react with redox-active iron minerals and/or dissolved Fe^{2+} and various nitrogen sources to form amino acids, alpha-hydroxy acids (αHA's), thiols, and other citric acid cycle intermediates (Barge et al., 2019; Huber & Wächtershäuser, 2003; Muchowska et al., 2017, 2019; Novikov & Copley, 2013). The amino acids and αHA's formed in these reactions can then polymerize to form larger functional molecules (Forsythe et al., 2015, 2017). From previous studies, it is clear that minerals are important for driving abiotic reactions of these two precursors to synthesize a variety of prebiotically relevant products. However, it is not known how the specific geological conditions could affect the *relative* abundances of products, which in turn might affect the composition and function of any oligomers formed from this monomer seed reservoir (e.g., Chandru et al., 2018; Surman et al., 2019). Also, for astrobiology and planetary science where specific organic distribution patterns are sometimes considered a possible biosignature to search for life on other worlds (Creamer et al., 2017; Georgiou, 2018; Lovelock, 1965; McKay, 2011), it is important to consider whether environmentally directed abiotic organic reaction networks might also produce similar effects.

Previously it has been shown that pyruvate, when reacted with different transition metal sulfide (including iron, arsenic, zinc, and copper sulfide) minerals, gave different distributions of organic products (Novikov & Copley, 2013). In a recent study, we showed that the relative yields of products formed from pyruvate reacting with iron hydroxide minerals could be controlled by systematically varying the Fe(II)/Fe(III) ratio in the mineral as well as the pH (Barge et al., 2019). This suggests that redox, pH, and perhaps other environmental parameters could have a significant effect on the organic distribution patterns produced from prebiotic organic-mineral reactions. However, the reaction networks of pyruvate and glyoxylate have not been explored in this context, and it is also unknown what other conditions might be important. For example, the concentration of nitrogen (e.g., NH_3/NH_4^+) must be a factor for amino acid formation from either pyruvate or glyoxylate. However, in previous studies of reductive amination with iron hydroxides, very high concentrations of NH_3/NH_4^+ were used that are probably unrealistic for most geological settings (Barge et al., 2019; Huber & Wächtershäuser, 2003), so it is not known whether amino acid formation would still occur in these systems at lower, more environmentally realistic [NH_3/NH_4^+] values.

In this study, we investigated how the organic product distribution pattern of a prebiotic pyruvate/glyoxylate reaction network in the presence of iron minerals was affected by changing geochemical parameters (of iron mineral redox state, pH, and NH_3/NH_4^+ concentration). These are environmental parameters that could vary within a variety of planetary settings relevant for the emergence of life: Including in iron-rich subsurface or seafloor sediments where the upper layers may be more oxidizing than lower layers, or in hydrothermal vent chimneys where the interior reducing fluid interfaces with more oxidizing seawater (e.g., Martin et al., 2008). Iron oxyhydroxide minerals, which we used in these experimental simulations as a representative geochemical reactant and/or catalyst, are very sensitive to oxidation and can exist in a variety of redox states depending on local chemistry and pH (Halevy et al., 2017; Jolivet et al., 2004). In aqueous iron-rich systems such as early Earth's oceans and early/present day Mars, reactive iron oxyhydroxide minerals (such as green rust, magnetite, or ferric hydroxide) would be prevalent (Halevy et al., 2017). Iron mineral redox gradients can also coexist with gradients of pH, for example, in an early Earth hydrothermal system with alkaline vent fluid feeding into a more acidic, CO_2-rich ocean (Russell & Hall, 2006), or on Mars where iron-bearing minerals have formed in both acidic and alkaline conditions (Ehlmann et al., 2011; Murchie et al., 2009). Thus, a variety of combinations of redox, pH, and chemical concentrations could exist in planetary systems of interest and it is important to understand to what extent this would affect abiotic organic chemistry.

A primary consideration in this study was to simulate pyruvate and glyoxylate reactions in realistic geological systems relevant to early Earth environments as well as to chemically diverse organic/mineral samples likely to be encountered on other worlds such as Mars, Ceres, or Enceladus (De Sanctis et al., 2017; Michalski et al., 2018; Postberg et al., 2018). Iron is an important reactant in abiotic systems, and early Earth's ocean was rich in dissolved Fe^{2+} (with some minor Fe^{3+} content) (Shibuya et al., 2016). This iron could have precipitated as a variety of reactive oxide/hydroxide minerals with different Fe(II)/Fe(III) ratios.

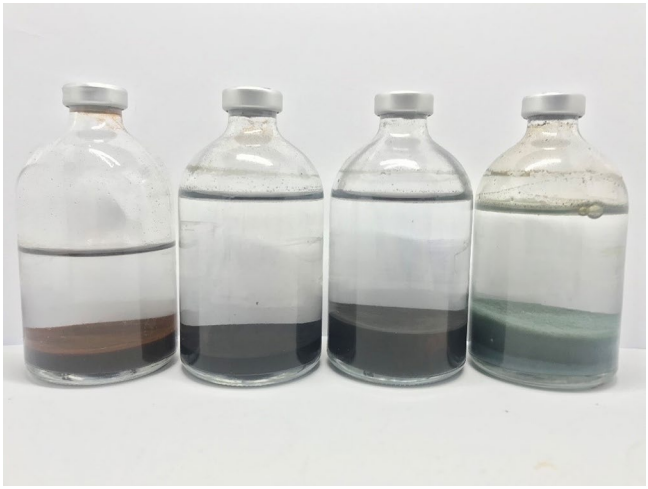

Figure 1. Iron hydroxide mineral precipitates formed at various Fe(II):Fe(III) ratios. Left to right: 100% Fe(III), 50% Fe(II), 75% Fe(II), and 100% Fe(II).

Metallic iron (Fe^0) is also highly reactive with these organic precursors (Muchowska et al., 2017) but was not as abundant in early/present-day Mars or early Earth surface environments, so was not included in the experiments discussed here. However, in a chondrite system such as the subseafloor of Enceladus, Fe^0 might play a larger role (Sekine et al., 2015). The employed pH range was chosen to span a range from neutral to alkaline, to simulate water-rock systems that are thought to be significant for producing energy for life or the origin of life on other worlds (Price et al., 2017; Russell et al., 2010, 2014; Tosca et al., 2018). NH_4Cl was used as the nitrogen source since NH_3/NH_4^+ is geologically realistic for early Earth (Stirling et al., 2016; Summers & Chang, 1993), with NH_3/NH_4^+ in equilibrium based on pH. Additionally, NH_3/NH_4^+ could be produced from abiotic NO_x reduction on Mars (Summers et al., 2012), and has been detected on Enceladus and Ceres (De Sanctis et al., 2015; Waite et al., 2009). We used a range of [NH_4Cl] from 0 to 375 mM to encompass likely planetary environments where these reactions might occur.

2. Materials and Methods

All reactions were carried out in a nitrogen-filled glove box. Solutions were prepared with Milli-Q water (18.2 MΩ•cm) that had also been purged with nitrogen or argon gas to remove any dissolved oxygen. The iron oxyhydroxide minerals representing minerals formed in a seafloor or wet sediment (Figure 1) were prepared using $FeCl_2•4H_2O$ and $FeCl_3•7H_2O$ where the total iron concentration in each serum bottle was 50 mM. The amount of Fe(II) and Fe(III) varied depending on the desired mole fraction of Fe(II):Fe(III) and no iron was added for experiments that did not contain any mineral. NH_3/NH_4^+ was introduced into the reaction by addition of ammonium chloride (NH_4Cl) ranging from 0 to 375 mM. Glyoxylate or pyruvate (glyoxylic acid monohydrate and/or sodium pyruvate) was added at a concentration of 2.5 mM. Milli-Q water was added to dissolve all reactants and 5 ml of 1 M NaOH was added to precipitate with the iron to synthesize an iron oxyhydroxide mineral. Each solution was then titrated with 1 M HCl or 1 M NaOH to pH 7 or 10. Each vial was placed in a water bath set to 70°C for 3 weeks and sampled at $t = 0$, 24 h, 48 h, 72 h, 1 week, 2 weeks, and/or 3 weeks. Five 1-ml aliquots were taken at each time point while agitating the bottles to ensure an even distribution of liquid and solid in each sample. 0.5 ml of 1 M NaOH was added to each aliquot to precipitate out the iron from solution. The samples were centrifuged and the supernatant was transferred to a new Eppendorf tube. Three samples were analyzed directly, the fourth sample was spiked with the amino acid, and the fifth with the α-hydroxy acid to verify their presence/absence.

2.1. ^{1}H Nuclear Magnetic Resonance Spectroscopy

To prepare the samples for liquid ^{1}H nuclear magnetic resonance (NMR) spectroscopy, the iron was first removed from solution via precipitation with 1 M NaOH. Unless otherwise described 0.54 ml of each sample was pipetted into a NMR tube along with 60 μl of sodium trimethylsilylpropanesulfonate (DSS)/D_2O standard. DSS was an efficient standard as its main peak appears at 0.00 ppm and does not interfere with any of the starting material or product peaks. The samples were analyzed on a 400 MHz Bruker equipped with an auto sampler. The ^{1}H NMR spectra were analyzed with MestReNova NMR analysis software. The concentrations of glyoxylate, pyruvate and their products are expressed as the combined methyl region peak areas for each molecule, relative to the normalized DSS peak. Data are plotted as the average of the three triplicate samples at a given time point in an experiment with error bars indicating the standard deviation. A complete list of experiments is found in Table S1. In many samples, we also observed an unidentified peak at 3.81 ppm and so a range of standards were run for identification of this peak (including iminodiacetic acid, diglycolic acid, glycinamide, MeOH, citric acid, and gly-gly).

2.2. Quadrupole Time-of-Flight Mass Spectrometry Analysis

Organic products were verified using quadrupole time-of-flight mass spectrometry (Q-TOF/MS). Reaction samples were stored at room temperature for short-term storage, and at −20°C for long-term storage. If the samples were frozen, they were brought to room temperature on the benchtop. The samples were vortexed for ∼1 min to ensure proper mixing. Three hundred microliters of sample was transferred to a high performance liquid chromatography vial and 0.2 μl was directly injected to an Agilent 6545 Q-TOF fitted with an Agilent InfinityLab Poroshell 120 HILIC-Z, 2.1 × 100 nm column for analysis. All samples were run five times. The samples were analyzed with Mass Hunter Profinder Professional and the identified compounds were matched to the Agilent METLIN metabolomics database. The identified compounds are summarized in Table S2.

2.3. Ligand Dissociation Experiments

We attempted ligand dissociation experiments to detect organics that were trapped in the mineral solid phase, as was suspected by the C fraction detected in the solids via combustion in our previous work (Barge et al., 2019), and to see if any polymers had formed. The reaction mixture of a 33% Fe^{2+} glyoxylic acid experiment (pH = 10, T = 70°C) was decanted and washed. The remaining mineral was then lyophilized and 30 mg of the mineral was placed in a Falcon tube. The mineral was then exposed to either 2 ml of pH = 7 H_2O (as a control), 2 ml of pH = 7 H_2O with 0.3 weight % phenanthroline (to test precipitated mineral), or 2 ml of pH = 3 H_2O with 0.3 weight % phenanthroline (to test dissolved mineral). These reactions were tested at two different temperatures: Room temperature or 70°C. The pH = 3 solutions were titrated with 1 M HCl. In the vials with phenanthroline, a red color was observed, indicating metal binding to the phenanthroline. ^{1}H NMR was taken at t = 0 and t = 1 week.

2.4. Mineral Analysis: XRD and Colorimetry

X-ray diffraction (XRD) analysis was conducted on the solid portion of a set of pH 10 glyoxylate experiments, at %Fe(II) = 0, 33, 50, and 100 after the experiments had run for 72 h. After completion of each reaction, the supernatant was discarded. The remaining minerals were lyophilized and stored in the glovebox. Prior to analysis, the samples were crushed with a ceramic mortar and pestle. The samples were loaded onto a 1.5 cc sample holder with a spatula and sealed with a Kapton film, and placed in the instrument with a copper anode. The samples were run on a Malvern Panalytical Aeris XRD. The spectra were compared to the RRUFF database (Lafuente et al., 2015) and the literature for identification (see supporting information).

Iron colorimetry analysis was conducted on the solid and liquid portions of pH 7 and 10 glyoxylate experiments, at %Fe(II) = 33, 50, 75, and 100. This technique was used to find the relative mole fractions of Fe(II) and Fe(III) in a 1-ml sample and in the supernatant. For supernatant samples, one extra sample was taken at t = 0 to which 0.5 ml of H_2O was added, the sample was centrifuged, and the supernatant was transferred to a new Eppendorf tube. For both pH 7 and 10 reactions, three extra samples were taken at t = 0 to which 0.5 ml of 2.5 M HCl was added to dissolve the solid. The same was done for t = 3 weeks' samples. All samples were diluted to 2 ml, where 1 ml was used for Fe(II) and 1 ml was used for Fe(total). To the Fe(II) samples, 100 μl of dH_2O was added and to the Fe(total) samples, 100 μl of 0.8 M ascorbic acid was added to reduce Fe(III) to Fe(II) since the colorimetry technique only measures Fe(II). After 10 min, 100 μl of 1 M HCl, 100 μl of 1 M sodium acetate, and 2 ml of 0.3% 1,10 phenanthroline were added to every sample while agitating the vials in between each reagent; the total assay volume was 3.3 ml. The samples were set aside for 10 min to let the color fully develop and were analyzed with a Thermo Fisher GENESYS 30 Visible spectrophotometer set to a wavelength of 510 nm.

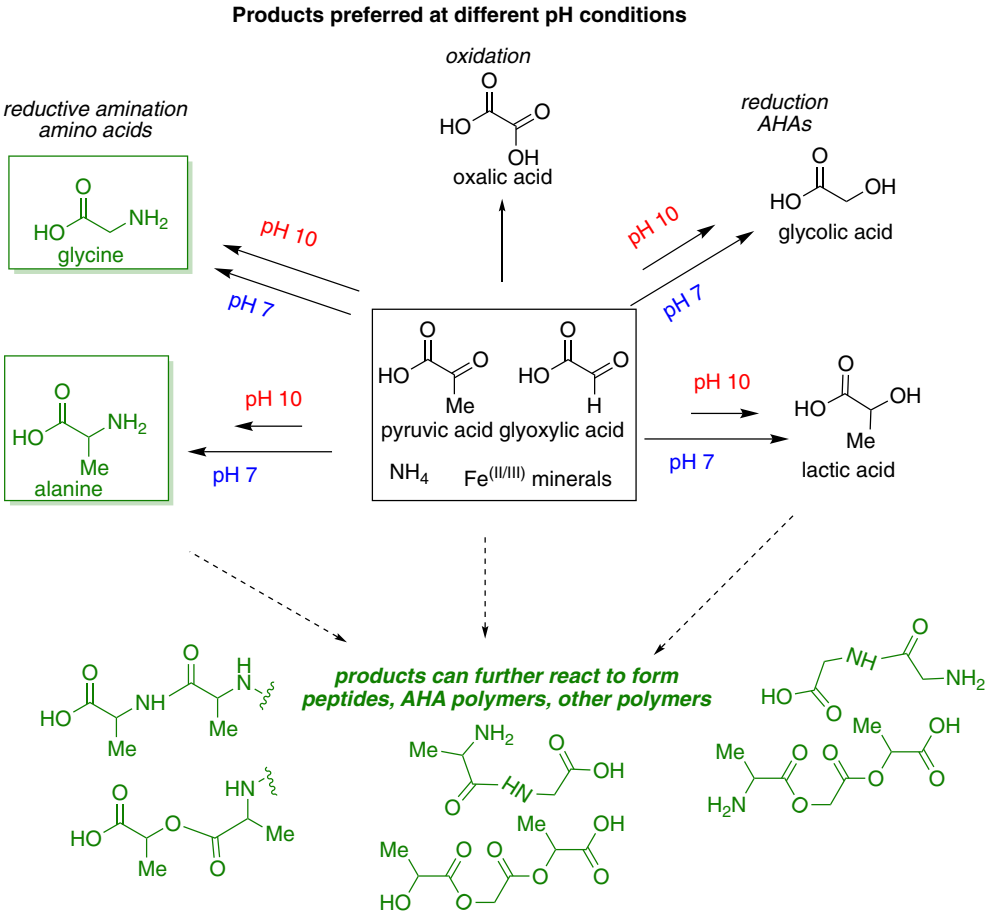

Figure 2. Reaction pathways of pyruvate (pyruvic acid) and glyoxylate (glyoxylic acid) with ammonia and iron minerals that were observed based on different pH conditions, and proposed larger molecules that might result from these monomers.

3. Results and Discussion

We observed that iron oxyhydroxide minerals played a large role in driving reactions of pyruvate and glyoxylate (Figure 2), and the relative yields of organic products observed from an experiment were dependent on the environmental parameters of pH, Fe(II)/Fe(III), and [NH_4Cl]. The main products we observed by ^{1}H NMR spectroscopy were amino acids (glycine and alanine) and αHA's (glycolate and lactate), validated by spiking with authentic standards and confirmed by LC-QTOF-MS. In the case of glyoxylate, other products were also observed by LC-QTOF-MS that were undetectable by ^{1}H NMR spectroscopy, including oxalate. There was also a ^{1}H NMR peak at 3.81 ppm that we were unable to identify (see supporting information). The 3.81 ppm peak was observed without any iron mineral present, and we hypothesize that it was a by-product of glyoxylate. This peak could correspond to an oligomer of glyoxylate, which can be formed under basic conditions with ammonia as a catalyst (Hoefnagel et al., 1992).

Glyoxylate reacted slowly with NH_4Cl in aqueous solution, producing glycine at and above ~10 mM NH_4Cl, as well as minor glycolate, over 3 weeks. Below ~200 mM NH_4, glyoxylate was still recovered at the end of the experiment, and the amount of glyoxylate remaining after 21 days decreased with increasing [NH_4Cl] (see supporting information). This is distinct from the pyruvate reaction system, we previously studied (Barge et al., 2019) where no reaction was observed when no minerals were present.

In contrast, when iron oxyhydroxide minerals were added, more pyruvate and glyoxylate reactions were possible (and glycine and glycolate, which were also formed with no mineral, were formed significantly

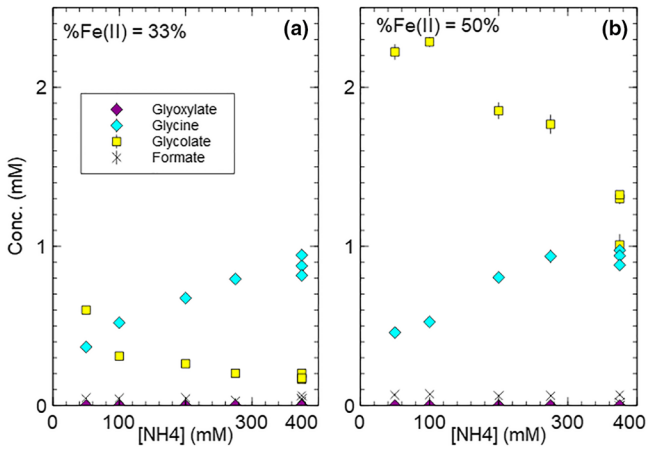

Figure 3. ^{1}H NMR results of glyoxylate reactions with Fe-oxyhydroxide minerals as a function of [NH_4Cl] at different Fe oxidation states; T = 70°C, pH 10: (a) Mineral containing 33% Fe(II) at t = 1 week. (b) Mineral containing 50% Fe(II) at t = 1 week. NMR, nuclear magnetic resonance.

faster). Over a period of several weeks, we observed formation of amino acids (alanine or glycine) and αHA's (lactate or glycolate) (Figures 3–5). (Acetate and formate were also observed in most pyruvate and glyoxylate reactions, respectively, but at very low concentration, and their yield did not vary with any of the conditions tested in experiments with minerals, so we cannot be confident they are not reagent contaminants and so do not report them as products.) When minerals were included, glyoxylate was almost always completely consumed after 21 days; whereas sometimes, depending on conditions, pyruvate still remained at the end of a 21-day experiment. The iron hydroxide minerals themselves likely had varied mineralogies, depending on pH and %Fe(II) (Jolivet et al., 2004). We did not observe significant oxidation of the Fe in the minerals (by colorimetry) over the 3-week reaction period. Even though magnetite, which is a more oxidized iron mineral phase, was detected in XRD in our samples, we believe this is an effect of oxidation during analysis; see supporting information.

Based on the different reactivity of glyoxylate and pyruvate, we varied several key geochemical parameters to determine how the organic distribution pattern of the products could be adjusted as a function of environmental conditions. In general, a higher concentration of [NH_4Cl] increased the amount of glycine relative to glycolate, and the presence of minerals increased the total glycine yield; this was true at various %Fe(II) compositions (Figure 3). However, at a given [NH_4Cl] the effect of the mole fraction of Fe(II) in the Fe-oxyhydroxide mineral, as well as the effect of pH, was significant (Figures 4 and 5). When looking at the relative yield of glycine and glycolate, the redox and pH conditions affected which product was dominant. Under alkaline conditions (pH 10), and with very reducing minerals (%Fe(II) = 90%–100%), glycolate was dominant and hardly any glycine was produced. This is similar to our previous results in the pyruvate reaction system (Barge et al., 2019), where above about 75% Fe(II), the αHA lactate was the dominant product over the amino acid alanine. When the iron oxyhydroxide mineral contained about 50% Fe(II), glycine and glycolate were produced at roughly equal abundances, which is also distinct from the pyruvate reaction system (Barge et al., 2019) where alanine dominated over lactate at this condition. In experiments with mixed glyoxylate and pyruvate, the expected relative distributions of amino acids and αHA's were observed relative to the amount of precursor that was initially included; a mixed precursor system did not yield any observable rate differences from a single precursor system.

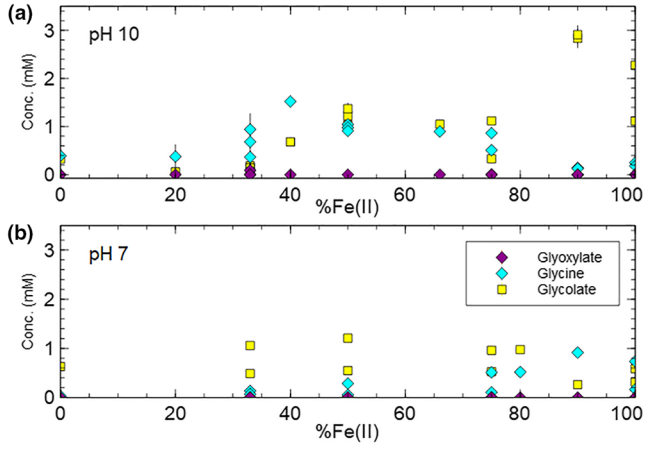

Figure 4. Results of glyoxylate reactions with Fe-oxyhydroxide minerals over the full iron redox gradient showing mM concentrations of the products detected at (a) pH 10 and (b) pH 7. The initial concentration of glyoxylate was 2.5 mM. ([NH_4Cl] = 375 mM; T = 70°C; sampled at t = 3 weeks).

We also observed that the relative abundance of products in the glyoxylate system in the iron redox gradient was strongly affected by pH (Figure 4). At pH 7, with reduced iron minerals, both glycine and glycolate were present, but when the minerals were more oxidized, glycolate was the dominant product (and glycine was a minor product) with the exception of Fe(II) = 90% where the yield of glycine was higher than glycolate. This is in contrast to the glyoxylate results at pH 10 where reduced minerals tended to favor glycolate synthesis and oxidized minerals favored both glycine and glycolate synthesis. In the pyruvate system, at pH 7, lactate was the only product observed and its concentration increased with %Fe(II); alanine was only formed under alkaline conditions and at intermediate %Fe(II) values (Figure 5).

Though this reaction system started with only two simple precursors, pyruvate and glyoxylate, a variety of organic distribution patterns were produced depending on the %Fe(II) in the mineral, the pH, and [NH_4Cl]—in other words, by varying the specific geochemical parameters of this aqueous mineral system (Figure 6). Determining the mechanisms of all the organic reactions is beyond the scope of this study.

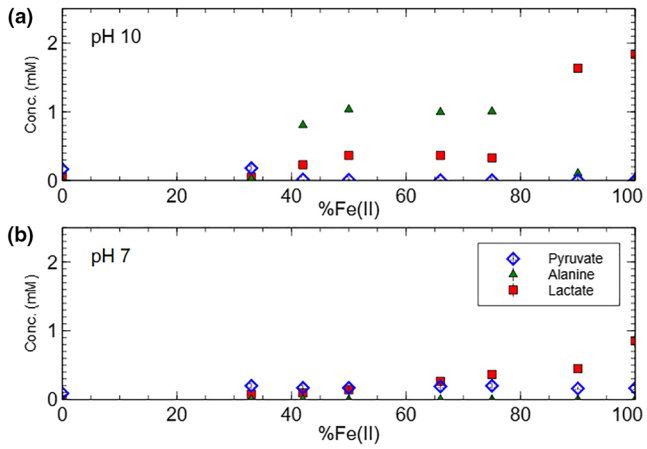

Figure 5. Results of pyruvate reactions with Fe-oxyhydroxide minerals over the full iron redox gradient showing mM concentrations of the products detected at (a) pH 10 and (b) pH 7. The initial concentration of pyruvate was 2.5 mM. ([NH_4Cl] = 375 mM; T = 70°C; sampled at t = 3 weeks).

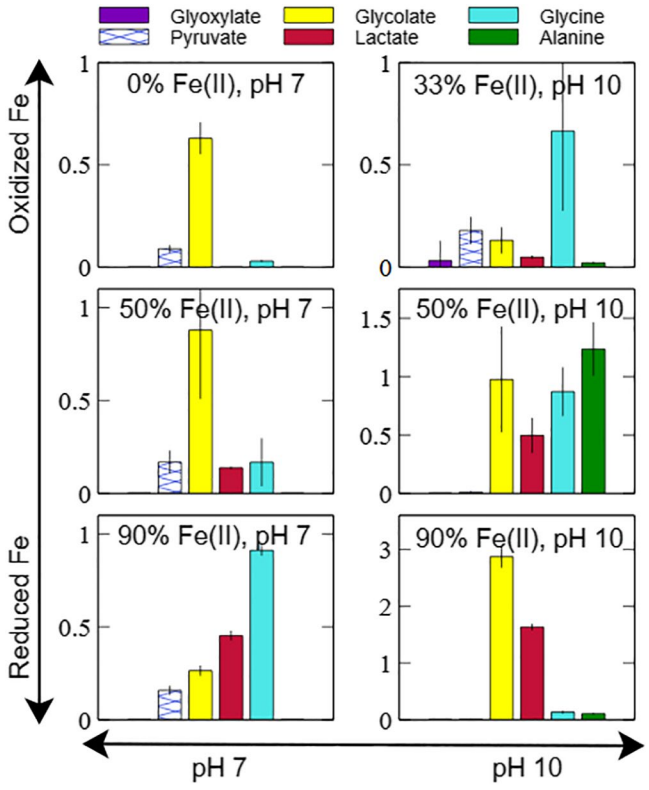

Figure 6. Organic distribution signatures for mineral-driven reactions at different redox and pH conditions. mM abundances of the organic precursors and products (after 21 days, at 375 mM [NH_4Cl]) are shown, at approximate values of fluid pH and %Fe(II) in the iron hydroxide mineral, showing how the organic distribution pattern is highly dependent on environmental parameters.

However, it seems likely that Fe(II) is a strong reductant for pyruvate to form lactate, as lactate was observed in greatest abundance at 100% Fe(II); though perhaps Fe(II) is not as important in glycolate formation from glyoxylate, since glycolate is observed at various %Fe(II) values. It is possible that the reduction of glyoxylate in the absence of Fe(II) may be due to a Cannizzaro reaction of glyoxylate, forming both glycolate (Figure S5) and oxalate (which is undetectable in ^{1}H NMR, but was observed via Q-TOF/MS in some of our experiments) (Butch et al., 2013; Geissman, 1944). The presence of Fe(II) in minerals in our experiments seems to facilitate reduction, since more αHA's are formed at intermediate to high %Fe(II); it is likely that the minerals are acting as reactants (rather than catalysts), though we were not able to determine the stoichiometry of the reaction. If Fe(II) in minerals was acting as a reductant, then we would expect to observe oxidation of Fe proportional to the reduction of pyruvate or glyoxylate over the course of the experiment. We did not observe significant iron oxidation after 21 days at any condition tested (Figure S23). However, under our experimental conditions there was a 20-fold excess of iron compared to the original amount of organic added, so even assuming complete stoichiometric iron oxidation we would only see a 5% change in [Fe(II)], which is within the range of error in our colorimetry technique. In a geological sample, there would also likely be an excess of minerals compared to organics, so the ability to determine whether iron minerals are acting as reactants versus catalysts in a planetary environment would depend on precision of techniques available to measure Fe(II)/Fe(III) (as well as organic detection). The effect of pH on alanine formation (increased at alkaline conditions) is likely due to the pK_a of ammonia at ~9.25, and so at pH 10, NH_3 (a stronger nucleophile) is more abundant and reactive. The precise mechanism of glyoxylate/pyruvate reductive amination to glycine/alanine in these systems was not established. One possibility is that an imine intermediate, followed by reduction of the C=N bond to form the amino group, was responsible for the synthesis (Gomez et al., 2002). In this regard, condensation to form the imine would be easier to form glycine due to the aldehyde starting material. However, we were unable to detect such an imine intermediate, which in any case is expected to be ephemeral given its high reactivity.

Other studies have shown that these amino acids and αHA's can react to form polymers, leading the system toward increased complexity. For example, long oligomers of lactate and glycolate can be produced from wet-dry cycling at temperatures as low as 30°C, and these can produce vast combinatorial libraries (Chandru et al., 2018). The combination of amino acids and αHA's is also significant. When αHA's including lactate and/or glycolate are mixed with alanine and/or glycine and undergo wet-dry cycles, depsipeptides are formed that can reach increasing amino acid content, and minerals can play a role in sequence selection (Doran et al., 2019; Forsythe et al., 2017, 2015; McKee et al., 2018). It has also recently been shown that αHA's can spontaneously form prebiotic compartments (Jia et al., 2019). Though these experimental prebiotic studies of monomer and oligomer formation vary in the environmental conditions employed (aqueous reactions vs. wet-dry cycles), it is possible that planetary environments exist that could facilitate both monomer synthesis as well as reactions to more complex organic molecules. As one example, iron precipitation in an aqueous environment can form

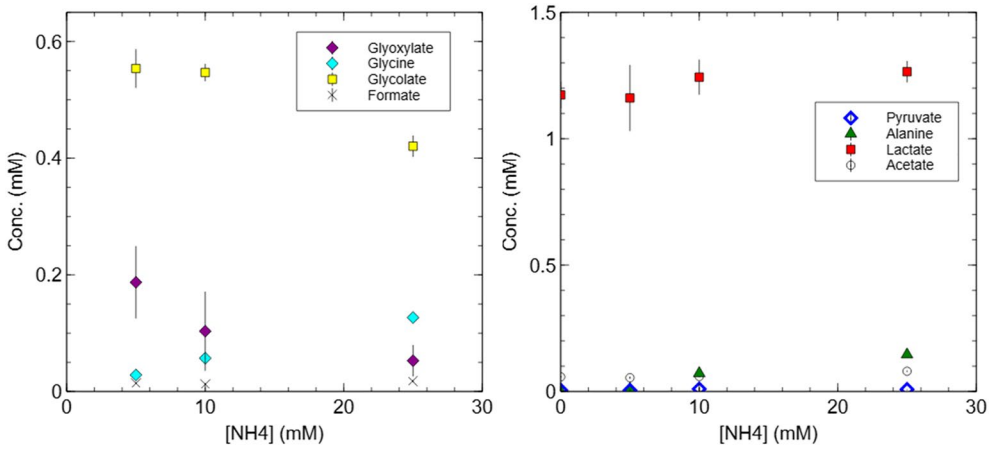

Figure 7. Glycine and alanine synthesis under low [NH_4Cl] conditions. Left: Glyoxylate reactions with iron hydroxide minerals (33% Fe(II)); Right: Pyruvate reactions with iron hydroxide minerals (50% Fe(II)); both at 70°C, pH 10, $t = 1$ week.

iron hydroxide minerals similar to the precipitates formed in our experiments, but can also form iron-silica gels as precursors to hydrothermal/sedimentary precipitates (Grenne & Slack, 2003; Hopkinson et al., 1988; Oehler, 1976; Tosca et al., 2016; Zheng et al., 2016); these silica/iron-silica gels can form lower water activity environments that might be beneficial for facilitating abiotic/prebiotic organic reactions (Gorrell et al., 2017; Pierre, 2020; Quinson et al., 1988; Trevors & Pollack, 2005; Westall et al., 2018). Hydrated silica-rich materials are present on Mars, and these may represent hydrothermal or other aqueous alteration environments that could also contain iron oxyhydroxides (Pineau et al., 2020; Schindler et al., 2019; Sun & Milliken, 2018; Tosca et al., 2018); in the case of potential Martian hot spring environments (e.g., Ruff et al., 2020; Sun & Milliken, 2020), it is especially possible that variations in temperature or water activity over time could have facilitated both aqueous reactions as well as those dependent on wet-dry cycles. It is also possible that complex abiotic/prebiotic chemistry on planets could be facilitated by multiple, interconnected environmental settings with varying conditions over space and time (Stüeken et al., 2013). The full condition space that can support complex molecule formation from glyoxylate and pyruvate, and the sum of planetary environments where such conditions may be found, is not well understood. However, it is likely that the environmental parameters that drive the initial distribution of amino acid and αHA monomers from these precursors will provide an additional chemical pressure to shape the composition and function of any oligomers/polymers formed from that seeding reservoir.

Previous work on prebiotic amino acid formation via reductive amination using NH_3/NH_4^+ as the N source has utilized a relatively large (>100-fold) excess of NH_3/NH_4^+ (Barge et al., 2019; Huber & Wächtershäuser, 2003). In this work, we examined an array of [NH_4Cl] values from 0 up to 375 mM, and we observed formation of glycine and alanine in mineral-containing experiments even at 5 mM [NH_4Cl] (the lowest NH_4Cl concentration tested; alanine was present at 0.0092 mM) (Figure 7). Other nitrogen sources in addition to NH_4Cl have been tested for prebiotic reductive amination in previous studies, including ammonium bicarbonate (NH_4HCO_3), hydrazine (NH_2NH_2), methylamine (CH_3NH_2), hydroxylamine hydrochloride ($NH_2OH{\bullet}HCl$), and dimethylamine ($(CH_3)_2NH$) (Huber & Wächtershäuser, 2003; Muchowska et al., 2017, 2019), some of which may be relevant for amino acid synthesis on other worlds. For example, nitriles, amines, imines, and various other nitrogen species have been detected on Titan (Loison et al., 2015); a variety of nitrogenous compounds are found in meteorites including methylamine, ammonia (Pizzarello and Williams, 2012; Pizzarello et al., 2011), aliphatic amines, and amino acids (Aponte et al., 2017; Pizzarello et al., 1994); ammonia and nitriles have been found in the plumes and E-ring of Enceladus (Postberg et al., 2008; Waite et al., 2009); and ammonium chloride and/or carbonate have been observed on Ceres (De Sanctis et al., 2016). NH_3/NH_4^+, being one of the simplest and most abundant reduced N sources, could also be formed from reducing NO_x species with iron or iron minerals on terrestrial planets such Mars or early Earth (Hansen, Borggaard, & Sorensen, 1994; Stern et al., 2015; Summers & Chang, 1993; Summers et al., 2012).

In our previous work with the pyruvate system, we found via combustion analysis that over 50% of the total C in a representative experiment was present in the minerals (Barge et al., 2019). We also observed in these experiments that a large fraction of organics is "missing" from the liquid phase and must therefore be concentrated in the minerals. The total amount of organics in the solid phase is greater at pH 7 than at pH 10, and at pH 10 is greater when the Fe minerals are more oxidized (see supporting information). We conducted ligand dissociation experiments on select solid samples to investigate organics in the minerals, but while small (less than 0.01 integration) aliphatic peaks corresponding to glycolate and glycine were visible, no polymers or additional products were observed in the reaction (see supporting information). However, extracting polar, highly functionalized organic compounds from minerals is challenging and more study is required to understand if polymerization is occurring in the solid phase in these experiments.

In a planetary environment, the parameters we tested as well as other geochemical conditions (such as mineralogy) may change with time and/or space, especially in gradient systems. In an open system, it is possible that water-soluble organic products formed at one set of conditions could diffuse to react at different conditions. Given that pH and %Fe(II) also seem to affect the degree to which organics are built up in the mineral during the initial reaction, it is possible that subsequent changes in environmental conditions such as fluid pH, or redox-driven mineralogical transformations could act to release previously bound organic products. In geological/planetary systems, there are various mechanisms that can subject the reaction to changes in water content, pH, and/or temperature, such as heat fluctuations in a hydrothermal system, tidal activity acting on a shallow vent system or surface water body, or impact-related heating of a subsurface environment. Further permutations of these organic products could be achieved by additional geological mechanisms such as photochemistry or volcanic heating (Guzman & Martin, 2010; Huber & Wächtershäuser, 2010; Saladino et al., 2011), or even re-generation of the glyoxylate and pyruvate precursors from their αHA's via iron-sulfur redox reactions (Wang et al., 2011). The specifics of which geochemical parameters and/or gradient conditions, and which corresponding monomer concentrations, are most favorable for polymerization and for driving certain depsipeptide/peptide functionalities remains to be investigated.

4. Conclusions

Geochemical environments could host a variety of possible combinations of environmental conditions, particularly in systems with overlapping redox/pH/chemical gradients. This would provide a complex and variable set of conditions for organic molecule synthesis in planetary environments. We have shown here that varying key geochemical parameters of iron mineral redox state, pH, and [NH_4Cl] can "tune" the organic distribution patterns produced from an abiotic reaction network of pyruvate and glyoxylate (Figures 2 and 3), two important precursors for the emergence of metabolism. Generally, increasing Fe(II) mole fraction relative to Fe(III) in the Fe-oxyhydroxide mineral led to increased αHA yield. As well, the pH had a pronounced effect on product distribution (amino acid vs. αHA) at a given %Fe(II). At any particular set of these geochemical conditions, pyruvate and glyoxylate did not give identical relative yields of their corresponding αHA and amino acid, so it is likely that other carboxylic acid precursors in these gradients also would act distinctly. In previous work, a large excess of NH_3/NH_4^+ has been utilized to drive reductive amination to form amino acids, and in this work we also observed that increasing [NH_4Cl] led to increased amino acid yield. However, our results showed that glycine and alanine can still be produced in the presence of iron oxhydroxide minerals even at much lower [NH_4Cl] concentrations (5 mM). Though organic compound distribution patterns have been considered a possible tool to identify biosignatures (Creamer et al., 2017; Georgiou, 2018; Lovelock, 1965; McKay, 2011), the field of prebiotic chemistry illustrates the high complexity and diversity that is possible in abiotic systems consisting of simple organic molecules, particularly with reactive minerals/ions that increase reaction network functionality. This abiotic organic reaction network occurs in the presence of iron minerals which are common and could exist in a variety of redox states on Mars, ocean worlds, and the early Earth; and under neutral to alkaline pH conditions that should be present in many planetary environments that experience mineral precipitation and alteration.

Data Availability Statement

The data from this study are available in the supporting information (XRD, colorimetry, representative NMR spectra, Q-TOF/MS), and a summary of the experimental data in the Open Science Framework (Barge, 2020).

Acknowledgments
This research was carried out at the Jet Propulsion Laboratory, California Institute of Technology, under a contract with NASA, supported by the NASA Astrobiology Institute (Icy Worlds), NASA-NSF Ideas Lab for the Origins of Life (Becoming Biotic), and JPL Research and Technology Development funds (Fate of Organics on Ocean Worlds). We thank Keith Billings (JPL) for XRD analysis, and the Dow Foundation Next Generation Fund for purchasing the Caltech 400 MHz NMR.

References

Aponte, J. C., Elsila, J. E., Glavin, D. P., Milam, S. N., Charnley, S. B., & Dworkin, J. P. (2017). Pathways to meteoritic glycine and methylamine. *ACS Earth and Space Chemistry*, *1*(1), 3–13. https://doi.org/10.1021/acsearthspacechem.6b00014

Barge, L. M. (2020). 2020-JGR-Planets-orgchem. Open Science Framework, AUPYZ. https://doi.org/10.17605/OSF.IO/AUPYZ

Barge, L. M., Flores, E., Baum, M. M., VanderVelde, D., & Russell, M. J. (2019). Redox and pH gradients drive amino acid synthesis in iron oxyhydroxide mineral systems. *Proceedings of the National Academy of Sciences of the United States of America*, *116*(11), 4828–4833. https://doi.org/10.1073/pnas.1812098116

Butch C., Cope E. D., Pollet P., Gelbaum L., Krishnamurthy R., Liotta C. L. (2013) Production of tartrates by cyanide-mediated dimerization of glyoxylate: A potential abiotic pathway to the citric acid cycle. *Journal of the American Chemical Society*, *135*, 13440–13445. https://doi.org/10.1021/ja405103r

Chandru, K., Guttenberg, N., Giri, C., Hongo, Y., Butch, C., Mamajanov, I., et al. (2018). Simple prebiotic synthesis of high diversity dynamic combinatorial polyester libraries. *Nature Communications Chemistry*, *1*, 30. https://doi.org/10.1038/s42004-018-0031-1

Cody, G. D., Boctor, N. Z., Filley, T. R., Hazen, R. M., Scott, J. H., Sharma, A., et al. (2000). Primordial carbonylated iron-sulfur compounds and the synthesis of pyruvate. *Science*, *289*, 1337–1340. https://doi.org/10.1126/science.289.5483.1337

Creamer, J. S., Mora, M. F., & Willis, P. A. (2017). Enhanced resolution of chiral amino acids with capillary electrophoresis for biosignature detection in extraterrestrial samples. *Analytical Chemistry*, *89*(2), 1329–1337. https://doi.org/10.1021/acs.analchem.6b04338

De Sanctis, M. C., Ammannito, E., McSween, H. Y., Raponi, A., Marchi, S., Capaccioni, F., et al. (2017). Localized aliphatic organic material on the surface of Ceres. *Science*, *355*(6326), 719–722. https://doi.org/10.1126/science.aaj2305

De Sanctis, M. C., Ammannito, E., Raponi, A., Marchi, S., McCord, T. B., McSween, H. Y., et al. (2015). Ammoniated phyllosilicates with a likely outer Solar System origin on (1) Ceres. *Nature*, *528*, 241–244. https://doi.org/10.1038/nature16172

De Sanctis, M. C., Raponi, A., Ammannito, E., Ciarniello, M., Toplis, M. J., McSween, H. Y., et al. (2016). Bright carbonate deposits as evidence of aqueous alteration on (1) Ceres. *Nature*, *536*, 54–57. https://doi.org/10.1038/nature18290

Doran, D., Abul-Haija, Y. M., & Cronin, L. (2019). Emergence of function and selection from recursively programmed polymerisation reactions in mineral environments. *Angewandte Chemie*, *131*(33), 11375–11378. https://doi.org/10.1002/ange.201902287

Eckhardt, A. K., Bergantini, A., Singh, S. K., Schreiner, P. R., & Kaiser, R. I. (2019). Formation of glyoxylic acid in interstellar ices: A key entry point for prebiotic chemistry. *Angewandte Chemie International Edition*, *58*, 5663–5667. https://doi.org/10.1002/anie.201901059

Eggins, B. R., Brown, E. M., McNeill, E. A., & Grimshaw, J. (1988). Carbon dioxide fixation by electrochemical reduction in water to oxalate and glyoxylate. *Tetrahedron Letters*, *29*(8), 945–948. https://doi.org/10.1016/S0040-4039(00)82489-2

Ehlmann, B. L., Mustard, J. F., Murchie, S. L., Bibring, J.-P., Meunier, A., Fraeman, A. A., et al. (2011). Subsurface water and clay mineral formation during the early history of Mars. *Nature*, *479*, 53–60. https://doi.org/10.1038/nature10582

Forsythe, J. G., Petrov, A. S., Millar, W. C., Yu, S.-S., Krishnamurthy, R., Grover, M. A., et al. (2017). Surveying the sequence diversity of model prebiotic peptides by mass spectrometry. *Proceedings of the National Academy of Sciences*, *114*(37), E7652–E7659. https://doi.org/10.1073/pnas.1711631114

Forsythe, J. G., Yu, S.-S., Mamajanov, I., Grover, M. A., Krishnamurthy, R., Fernández, R. M., et al. (2015). Ester-mediated amide bond formation driven by wet–dry cycles: A possible path to polypeptides on the prebiotic Earth. *Angewandte Chemie International Edition*, *54*, 9871–9875. https://doi.org/10.1002/anie.201503792

Geissman, T. A. (1944). The Cannizzaro reaction. In W. E. Bachmann, J. R. Johnson, L. F. Fieser, & H. R. Snyder (Eds.), *Organic reactions* (Vol. II, 2nd ed.). Hoboken, NJ: John Wiley & Sons, Inc. https://doi.org/10.1002/0471264180.or002.03

Georgiou, C. D. (2018). Functional properties of amino acid side chains as biomarkers of extraterrestrial life. *Astrobiology*, *18*, 11. https://doi.org/10.1089/ast.2018.1868

Gomez, S., Peters, J. A., & Maschmeyer, T. (2002). The reductive amination of aldehydes and ketones and the hydrogenation of nitriles: Mechanistic aspects and selectivity control. *Advances in Synthetic Catalysis*, *344*, 1037–1057.

Gorrell, I. B., Henderson, T. W., Albdeery, K., Savage, P. M., & Kee, T. P. (2017). Chemical transformations in proto-cytoplasmic media. Phosphorus coupling in the silica hydrogel phase. *Life*, *7*(4), 45. https://doi.org/10.3390/life7040045

Grenne, T., & Slack, J. F. (2003). Bedded jaspers of the Ordovician Løkken ophiolite, Norway: Seafloor deposition and diagenetic maturation of hydrothermal plume-derived silica-iron gels. *Mineralium Deposita*, *38*, 625–639.

Guzman, M. I., & Martin, S. T. (2010). Photo-production of lactate from glyoxylate: How minerals can facilitate energy storage in a prebiotic world. *Chemical Communications*, *46*, 2265–2267. https://doi.org/10.1039/B924179E

Halevy, I., Alesker, E., Schuster, E. M., Popovitz-Biro, R., & Feldman, Y. (2017). A key role for green rust in the Precambrian oceans and the genesis of iron formations. *Nature Geoscience*, *10*, 135–139. https://doi.org/10.1038/ngeo2878

Hansen, H. C. B., Borggaard, O. K., & Sørensen, J. (1994). Evaluation of the free energy of formation of Fe(II)-Fe(III) hydroxide-sulphate (green rust) and its reduction of nitrite. *Geochim Cosmochim Acta*, *58*, 2599–2608. https://doi.org/10.1016/0016-7037(94)90131-7

Hoefnagel, A. J., Van Bekkum, H., & Peters, J. A. (1992). The reaction of glyoxylic acid with ammonia revisited. *Journal of Organic Chemistry*, *57*(14), 3916–3921. https://doi.org/10.1021/jo00040a035

Hopkinson, L., Roberts, S., Herrington, R., & Wilkinson, J. (1988). Self-organization of submarine hydrothermal siliceous deposits: Evidence from the TAG hydrothermal mound, 26°N Mid-Atlantic Ridge. *Geology*, *26*(4), 347–350. https://doi.org/10.1130/0091-7613(1998)026<0347:SOOSHS>2.3.CO;2

Huber, C., & Wächtershäuser, G. (2003). Primordial reductive amination revisited. *Tetrahedron Letters*, *44*(8), 1695–1697. https://doi.org/10.1016/S0040-4039(02)02863-0

Huber, C., & Wächtershäuser, G. (2010). Synthesis of α-amino and α-hydroxy acids under volcanic conditions: Implications for the origin of life. *Tetrahedron Letters*, *51*(7), 1069–1071. https://doi.org/10.1016/j.tetlet.2009.12.084

Jia, T. Z., Chandru, K., Hongo, Y., Afrin, R., Usui, T., Myojo, K., et al. (2019). Membraneless polyester microdroplets as primordial compartments at the origins of life. *Proceedings of the National Academy of Sciences*, *116*(32), 15830–15835. https://doi.org/10.1073/pnas.1902336116

Jolivet, J. P., Chanéac, C., & Tronc, E. (2004). Iron oxide chemistry. From molecular clusters to extended solid networks. *Chemical Communications,* (5), 481–487. https://doi.org/10.1039/B304532N

Lafuente, B., Downs, R. T., Yang, H., & Stone, N. (2015). The power of databases: The RRUFF project. In T. Armbruster, R. M. Danisi (Eds.), *Highlights in mineralogical crystallography* (pp. 1–30). Berlin, Germany: W. De Gruyter.

Loison, J. C., Hébrard, E., Dobrijevic, M., Hickson, K. M., Caralp, F., Hue, V., et al. (2015). The neutral photochemistry of nitriles, amines and imines in the atmosphere of Titan. *Icarus*, *247*, 218–247. https://doi.org/10.1016/j.icarus.2014.09.039

Lovelock, J. E. (1965). A physical basis for life detection experiments. *Nature*, *207*, 568–570. https://doi.org/10.1038/207568a0

Marín-Yaseli, M. R., González-Toril, E., Mompeán, C., & Ruiz-Bermejo, M. (2016). The role of aqueous aerosols in the "Glyoxylate Scenario": An experimental approach. *Chemistry*, *22*(36), 12785–12799. https://doi.org/10.1002/chem.201602195

Martin, W., Baross, J., Kelley, D., & Russell, M. J. (2008). Hydrothermal vents and the origin of life. *Nature Reviews Microbiology*, *6*, 805–814. https://doi.org/10.1038/nrmicro1991

McKay, C. P. (2011). The search for life in our Solar System and the implications for science and society. *Philosophical Transactions of the Royal Society of London Series A*, *369*, 594–606. https://doi.org/10.1098/rsta.2010.0247

McKee, A. D., Solano, M., Saydjari, A., Bennett, C. J., Hud, N. V., & Orlando, T. M. (2018). A possible path to prebiotic peptides involving silica and hydroxy acid-mediated amide bond formation. *ChemBioChem*, *19*(18), 1913–1917. https://doi.org/10.1002/cbic.201800217

Michalski, J. R., Onstott, T. C., Mojzsis, S. J., Mustard, J., Chan, Q. H. S., Niles, P. B., et al. (2018). The Martian subsurface as a potential window into the origin of life. *Nature Geoscience*, *11*, 21–26. https://doi.org/10.1038/s41561-017-0015-2

Mohammed, F. S., Chen, K., Mojica, M., Conley, M., Napoline, J. W., Butch, C., et al. (2017). A plausible prebiotic origin of glyoxylate: Nonenzymatic transamination reactions of glycine with formaldehyde. *Synlett*, *28*(01), 93–97. https://doi.org/10.1055/s-0036-1588657

Muchowska, K. B., Varma, S. J., Chevallot-Beroux, E., Lethuillier-Karl, L., Li, G., & Moran, J. (2017). Metals promote sequences of the reverse Krebs cycle. *Nature Ecology & Evolution*, *1*, 1716–1721. https://doi.org/10.1038/s41559-017-0311-7

Muchowska, K. B., Varma, S. J., & Moran, J. (2019). Synthesis and breakdown of universal metabolic precursors promoted by iron. *Nature*, *569*, 104–107. https://doi.org/10.1038/s41586-019-1151-1

Murchie, S. L., Mustard, J. F., Ehlmann, B. L., Milliken, R. E., Bishop, J. L., McKeown, N. K., et al. (2009). A synthesis of Martian aqueous mineralogy after one Mars year of observations from the Mars Reconnaissance Orbiter. *Journal of Geophysical Research*, *114*(E2), E00D06. https://doi.org/10.1029/2009JE003342

Novikov, Y., & Copley, S. D. (2013). Reactivity landscape of pyruvate under simulated hydrothermal vent conditions. *Proceedings of the National Academy of Sciences*, *110*(33), 13283–13288. https://doi.org/10.1073/pnas.1304923110

Oehler, J. H. (1976). Hydrothermal crystallization of silica gel. *GSA Bulletin*, *87*(8), 1143–1152.

Pierre, A. C. (2020). Wet gels and their drying. In *Introduction to sol-gel processing*. Cham, Switzerland: Springer. https://doi.org/10.1007/978-3-030-38144-8_8

Pineau, M., Le Deit, L., Chauviré, B., Carter, J., Rondeau, B., & Mangold, N. (2020). Toward the geological significance of hydrated silica detected by near infrared spectroscopy on Mars based on terrestrial reference samples. *Icarus*, *347*, 113706.

Pizzarello, S., Feng, X., Epstein, S., & Cronin, J. R. (1994). Isotopic analyses of nitrogenous compounds from the murchison meteorite: Ammonia, amines, amino acids, and polar hydrocarbons. *Geochim. Cosmochim. Acta*, *58*(24), 5579–5587. https://doi.org/10.1016/0016-7037(94)90251-8

Pizzarello, S., & Williams, L. B. (2012). Ammonia in the early solar system: An account from carbonaceous meteorites. *The Astrophysics Journal*, *749*, 161. https://doi.org/10.1088/0004-637X/749/2/161

Pizzarello, S., Williams, L. B., Lehman, J., Holland, G. P., & Yarger, J. L. (2011). Abundant ammonia in primitive asteroids and the case for a possible exobiology. *Proceedings of the National Academy of Sciences of the United States of America*, *108*(11), 4303–4306. https://doi.org/10.1073/pnas.1014961108

Postberg, F., Kempf, S., Hillier, J. K., Srama, R., Green, S. F., McBride, N., et al. (2008). The E ring in the vicinity of Enceladus I. Probing the moon's interior—the composition of E ring particles. *Icarus*, *193*(2), 438–454. https://doi.org/10.1016/j.icarus.2007.09.001

Postberg, F., Khawaja, N., Abel, B., Choblet, G., Glein, C. R., Gudipati, M. S., et al. (2018). Macromolecular organic compounds from the depths of Enceladus. *Nature*, *558*, 564–568. https://doi.org/10.1038/s41586-018-0246-4

Price, R., Boyd, E. S., Hoehler, T. M., Wehrmann, L. M., Bogason, E., Valtýsson, H. Þ., et al. (2017). Alkaline vents and steep Na^+ gradients from ridge-flank basalts—implications for the origin and evolution of life. *Geology*, *45*(12), 1135–1138. https://doi.org/10.1130/G39474.1

Quinson, J. F., Tchipkam, N., Dumas, J., Bovier, C., & Serughetti, J. (1988). Drying evolution of wet silica gels. *Journal of Non-Crystalline Solids*, *100*, 231–235.

Ruff, S. W., Campbell, K. C., Van Kranendonk, M. J., Rice, M. S., & Farmer, J. D. (2020). The case for ancient hot springs in Gusev crater, Mars. *Astrobiology*, *20*(4), 475–499.

Russell, M. J., Barge, L. M., Bhartia, R., Bocanegra, D., Bracher, P. J., Branscomb, E., et al. (2014). The drive to life on wet and icy worlds. *Astrobiology*, *14*(4), 308–343. https://doi.org/10.1089/ast.2013.1110

Russell, M. J., & Hall, A. J. (2006). The onset and early evolution of life. In S. E. Kesler & H. Ohmoto (Eds.), Evolution of early Earth's atmosphere, hydrosphere, and biosphere—constraints from ore deposits. (Vol. 198, pp. 1–32). Memoir: Geological Society of America. https://doi.org/10.1130/2006.1198(01)

Russell, M. J., Hall, A. J., & Martin, W. (2010). Serpentinization as a source of energy at the origin of life. *Geobiology*, *8*(5), 355–371. https://doi.org/10.1111/j.1472-4669.2010.00249.x

Saladino, R., Brucato, J. R., De Sio, A., Botta, G., Pace, E., & Gambicorti, L. (2011). Photochemical synthesis of citric acid cycle intermediates based on titanium dioxide. *Astrobiology*, *11*(8), 815–824. https://doi.org/10.1089/ast.2011.0652

Schindler, M., Michel, S., Batcheldor, D., & Hochella, M. F., Jr. (2019). A nanoscale study of the formation of Fe-(hydr)oxides in a volcanic regolith: Implications for the understanding of soil forming processes on Earth and Mars. *Geochimica et Cosmochimica Acta*, *264*, 43–66.

Sekine, Y., Shibuya, T., Postberg, F., Hsu, H.-W., Suzuki, K., Masaki, Y., et al. (2015). High-temperature water-rock interactions and hydrothermal environments in the chondrite-like core of Enceladus. *Nature Communications*, *6*, 8604. https://doi.org/10.1038/ncomms9604

Shibuya, T., Russell, M. J., & Takai, K. (2016). Free energy distribution and hydrothermal mineral precipitation in Hadean submarine alkaline vent systems: Importance of iron redox reactions under anoxic conditions. *Geochim Cosmochim Acta*, *175*, 1–19. https://doi.org/10.1016/j.gca.2015.11.021

Stern, J. C., Sutter, B., Freissinet, C., Navarro-González, R., McKay, C. P., Archer, P. D., Jr., et al. (2015). Evidence for indigenous nitrogen in sedimentary and aeolian deposits from the Curiosity rover investigations at Gale crater, Mars. *Proceedings of the National Academy of Sciences*, *112*(14), 4245–4250. https://doi.org/10.1073/pnas.1420932112

Stirling, A., Rozgonyi, T., Krack, M., & Bernasconi, M. (2016). Prebiotic NH3 formation: Insights from simulations. *Inorganic Chemistry*, *55*(4), 1934–1939. https://doi.org/10.1021/acs.inorgchem.5b02911

Stüeken, E. E., Anderson, R. E., Bowman, J. S., Brazelton, W. J., Colangelo-Lillis, J., Goldman, A. D., et al. (2013). Did life originate from a global chemical reactor? *Geobiology*, *11*(2), 101–126.

Summers, D. P., Basa, R. C. B., Khare, B., & Rodoni, D. (2012). Abiotic nitrogen fixation on terrestrial planets: Reduction of NO to ammonia by FeS. *Astrobiology*, *12*(2), 107–114. https://doi.org/10.1089/ast.2011.0646

Summers, D. P., & Chang, S. (1993). Prebiotic ammonia from reduction of nitrite by iron (II) on the early Earth. *Nature*, *365*, 630–633. https://doi.org/10.1038/365630a0

Sun, V. Z., & Milliken, R. E. (2018). Distinct geologic settings of opal-A and more crystalline hydrated silica on Mars. *Geophysical Research Letters*, *45*(19) 10221–10228.

Sun, V. Z., & Milliken, R. E. (2020). Characterizing the mineral assemblages of hot spring environments and applications to Mars orbital data. *Astrobiology*, *20*(4), 453–474.

Surman, A. J., Rodriguez-Garcia, M., Abul-Haija, Y. M., Cooper, G. J. T., Gromski, P. S., Turk-MacLeod, R., et al. (2019). Environmental control programs the emergence of distinct functional ensembles from unconstrained chemical reactions. *Proceedings of the National Academy of Sciences*, *116*(12), 5387–5392. https://doi.org/10.1073/pnas.1813987116

Tosca, N. J., Ahmed, I. A. M., Tutolo, B. M., Ashpitel, A., & Hurowitz, J. A. (2018). Magnetite authigenesis and the warming of early Mars. *Nature Geoscience*, *11*, 635–639. https://doi.org/10.1038/s41561-018-0203-8

Tosca, N. J., Guggenheim, S., & Pufahl, P. K. (2016). An authigenic origin for Precambrian greenalite: Implications for iron formation and the chemistry of ancient seawater. *GSA Bulletin*, *128*(3/4), 511–530. https://doi.org/10.1130/B31339.1

Trevors, J. T., & Pollack, G. H. (2005). Hypothesis: The origin of life in a hydrogel environment. *Progress in Biophysics and Molecular Biology*, *89*(1), 1–8.

Varma, S. J., Muchowska, K. B., Chatelain, P., & Moran, J. (2018). Native iron reduces CO_2 to intermediates and end-products of the Acetyl-CoA pathway. *Nature Ecology & Evolution*, *2*, 1019–1024. https://doi.org/10.1038/s41559-018-0542-2

Waite, J. H., Lewis, W. S., Magee, B. A., Lunine, J. I., McKinnon, W. B., Glein, C. R., et al. (2009). Liquid water on Enceladus from observations of ammonia and 40Ar in the plume. *Nature*, *460*(7254), 487–490. https://doi.org/10.1038/nature08153

Wang, W., Yang, B., Qu, Y., Liu, X., & Su, W. (2011). FeS/S/FeS_2 redox system and its oxidoreductase-like chemistry in the iron-sulfur world. *Astrobiology*, *11*(5), 471–476. https://doi.org/10.1089/ast.2011.0624

Westall, F., Hickman-Lewis, K., Hinman, N., Gautret, P., Campbell, K. A., et al. (2018). A hydrothermal-sedimentary context for the origin of life. *Astrobiology*, *18*(3), 259–293.

Zheng, X.-Y., Beard, B. L., Reddy, T. R., Roden, E. E., & Johnson, C. M. (2016). Abiologic silicon isotope fractionation between aqueous Si and Fe(III)–Si gel in simulated Archean seawater: Implications for Si isotope records in Precambrian sedimentary rocks. *Geochimica et Cosmochimica Acta*, *187*, 102–122.

References From Supporting Information

Chitrakar, R., Tezuka, S., Sonoda, A., Sakane, K., Ooi, K., & Hirotsu, T. (2006). Phosphate adsorption on synthetic goethite and akaganeite. *Journal of Colloid and Interface Science*, *298*(2), 602–608. https://doi.org/10.1016/j.jcis.2005.12.054

Dodge, C. J., Francis, A. J., Gillow, J. B., Halada, G. P., Eng, C., & Clayton, C. R. (2002). Association of uranium with iron oxides typically formed on corroding steel surfaces. *Environmental Science & Technology*, *36*(16), 3504–3511. https://doi.org/10.1021/es011450+

Hari-Bala, X., Guo, Y., Zhao, X., Zhao, J., Fu, W., Ding, X., et al. (2006). Controlling the particle size of nanocrystalline titania via a thermal dissociation of substrates with ammonium chloride. *Materials Letters*, *60*(4), 494–498. https://doi.org/10.1016/j.matlet.2005.09.030

Wang, D., & Li, Z. (2011). Kinetic analysis for crystal growth rate of NH_4Cl in the NaCl-$MgCl_2$-H_2O system with a thermodynamic approach. *AIChE Reactors, Kinetics, and Catalysis*, *58*(3), 914–924. https://doi.org/10.1002/aic.12604